Recoverable Solution Reaction of HiPco Carbon Nanotubes with Hydrogen Peroxide

Chulho Song,[†] Pehr E. Pehrsson,[‡] and Wei Zhao*[,†]

Department of Chemistry, University of Arkansas, 2801 South University Avenue, Little Rock, Arkansas 72204, and Chemistry Division, Naval Research Laboratory, Washington, DC 20375-5000

Received: June 8, 2005; In Final Form: September 7, 2005

There is increasing interest in developing single-walled carbon nanotubes (SWNTs)-based optical biosensors for remote or in vitro and in vivo sensing because the near-IR optical properties of SWNTs are very sensitive to surrounding environmental changes. Many enzyme-catalyzed reactions yield hydrogen peroxide (H_2O_2) as a product. To our knowledge, there is no report on the interaction of H_2O_2 with SWNTs from the optical sensing point of view. Here, we study the reaction of H_2O_2 with an aqueous suspension of water-soluble (ws) HiPco SWNTs encased in the surfactant sodium dodecyl sulfate (SDS). The SWNTs are optically sensitive to hydrogen peroxide in pH 6.0 buffer solutions through suppression of the near-IR absorption band intensity. Interestingly, the suppressed spectral intensity of the nanotubes recovers by increasing the pH, by decomposing the H_2O_2 into H_2O and O_2 with the enzyme catalase, and by dialytically removing H_2O_2. Preliminary studies on the mechanisms suggest that H_2O_2 withdraws electrons from the SWNT valence band by charge transfer, which suppresses the nanotube spectral intensity. The findings suggest possible enzyme-assisted molecular recognition applications by selective optical detection of biological species whose enzyme-catalyzed products include hydrogen peroxide.

Introduction

Single-walled carbon nanotubes (SWNTs) have received much attention as potential electronic nanosensors.[1−6] However, because the SWNT optical properties are very sensitive to surrounding environmental changes,[7−20] there is also increasing interest in developing nanotubes-based *optical* biosensors for remote or in vitro and in vivo sensing. Previous work[7−17] has demonstrated that surface-modified water-soluble SWNTs are optically sensitive to pH changes in the near-infrared (IR) spectral range, which suggests their utility in near-IR optical pH-sensing applications. Water-soluble SWNTs (ws-SWNTs) can have an undisrupted characteristic band structure when coated with surfactants or polymers and prepared by mild surface functionalization.[9−25] These unique ws-SWNTs provide us with rich solution chemistry for further exploration. However, up to now, most SWNT sensor research work has focused on electronic devices because of their sensitive electrical response.[1−6] There has been comparatively little examination of the optical properties of SWNTs and their possible exploitation in enzyme-based detection of biological molecules. For example, many enzyme-catalyzed reactions yield hydrogen peroxide (H_2O_2) as a product[5,26−32] which enables electrochemical glucose sensing for diabetes diagnostics.[26−32] Although H_2O_2 has been used in purification of SWNTs,[33] we know of no research directly addressing its interaction with SWNTs for optical sensing. In addition, development of new optical tools for hydrogen peroxide detection is of physiological and pathological importance because H_2O_2 is a major reactive oxygen species in living organisms and has been implicated in aging and severe human diseases.[34] Recent progress in the development of nanolasers,[35] nanowaveguides,[36] and optical nanofibers[37] suggests the use of nanostructural materials as nanolight sources for optical nanosensors.[38] In this paper, we use a representative ws-SWNT system (HiPco SWNTs encased in the surfactant sodium dodecyl sulfate (SDS)) to study the SWNT solution reaction with H_2O_2. The near-IR optical transitions of semiconducting SWNTs show that H_2O_2 interacts with HiPco SWNTs through valence electron withdrawal, which suppresses the nanotube spectral intensity. The SWNTs respond optically to H_2O_2 at a detection limit of 11 μM. More intriguingly, the suppressed nanotube band intensity recovers when the H_2O_2 is decomposed into H_2O and O_2 with the enzyme catalyst catalase, by dialytically removing H_2O_2, and by increasing the solution pH. These findings set a solid foundation for H_2O_2-related optical sensing applications using surface-modified SWNTs and suggest an optical sensing method for important biological molecules.

Experimental Section

Materials. Raw HiPco SWNTs (lot no. 79, December 2, 2001) were purchased from Carbon Nanotechnologies, Inc. with sizes ranging from 0.7 to 1.1 nm in diameter and a few hundred nanometers long.[10] A TEM image of the SWNTs is shown in Figure 1S in the Supporting Information. The reagents SDS (>99% pure), H_2O_2 (30 wt %) and catalase (EC 1.11.1.6, 1870 units/mg) were from Sigma-Aldrich.

Preparation of SDS-Encased HiPco SWNT Solutions. Suspensions of nanotubes in 1 wt % SDS in H_2O were prepared using a procedure similar to that described in refs 10 and 39. Briefly, in a typical experiment, ~2.4 mg of pristine HiPco SWNTs was weighed on a microgram-scaled balance in a TGA and placed in a 10 mL test tube with 5 mL of 1 wt % SDS aqueous solution. Mild sonication was applied in an ultrasonic bath (Branson model 1510R-MT, 42 kHz, output power 70 W) for 1−3 min to disperse the nanotubes, and then the mixture was vigorously sonicated for about 1 min (longer sonication times may suppress the SWNT optical features[39]). Different

* Corresponding author. E-mail: wxzhao@ualr.edu. Phone: (501) 569-8823.
[†] University of Arkansas.
[‡] Naval Research Laboratory.

10.1021/jp053077o CCC: $30.25
Published on Web 10/20/2005

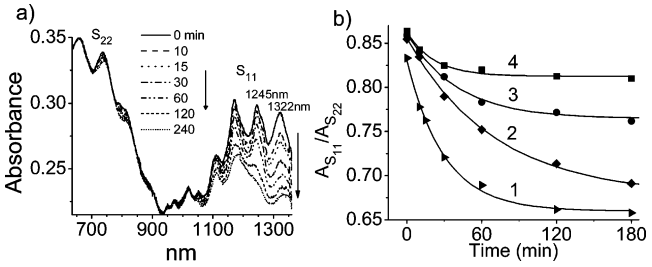

Figure 1. (a) Absorption spectra of SDS-encased HiPco SWNTs in a pH 6.0 buffer solution change as a function of time after addition of 30 ppm H_2O_2. (b) The ratio As_{11}/As_{22} of the absorbance of the 1322 nm S_{11} band and the 659 nm S_{22} band of the SDS-encased SWNT samples in different pH buffers (1, pH 6.0; 2, pH 7.0; 3, pH 8.0; 4, pH 9.0) is plotted as a function of time after addition of 30 ppm H_2O_2. The solid lines are exponential fits.

centrifuge speeds were used to get well-dispersed nanotube suspensions from the resulting mixture. It was observed that under a relatively low speed at ~1300*g*, the supernatant retained larger diameter nanotubes with an absorption band at 1322 nm. However, under a higher speed at ~16000*g*, the larger diameter nanotubes at 1322 nm in the supernatant decreased significantly (Figure 2S in the Supporting Information). Both supernatants presented a similar H_2O_2-dependent behavior (Figure 1 in the text, and Figure 2S in the Supporting Information). However, because the larger diameter nanotubes at 1322 nm with a smaller band gap are more sensitive to H_2O_2, in this report we concentrated on the supernatant obtained under the low-speed centrifuge. After 1 h of centrifugation of the resulting mixture (Sargent-Welch Scientific Co., ~1300*g*), 0.8 mL of the supernatant was decanted and diluted with about 0.8 mL of the SDS solution (the exact volume was determined by monitoring the absorbance at 1245 nm so that, after dilution, the absorbance was ~0.6). About 0.13 mL of the diluted SWNT solution was mixed with an equal amount of a pH 6.0 phosphate buffer (50 mM) to make a buffered SWNT solution or the SDS solution to make an unbuffered SWNT solution. The resulting solution was transferred into a 1 mm quartz cell for optical measurements. It had an optical absorbance of ~0.3 at 1245 nm at an HiPco nanotube concentration of about 0.1 mg/mL. The suspensions were stable during the measurement period of 24 h (Figure 3S in the Supporting Information).

The purity of the raw HiPco nanotubes may affect the spectral features and must be taken into account. Figure 4S in the Supporting Information shows that suspensions of raw HiPco nanotubes (r-SWNTs) recently purchased from Carbon Nanotechnologies, Inc. had less-resolved spectral features than those of the old HiPco nanotubes (o-SWNTs) prepared with low centrifuge speed and used in this work, probably because the r-SWNTs contained more impurities such as amorphous carbon than o-SWNTs. High-speed centrifugation was more efficient at removing impurities, since the suspensions of both raw HiPco nanotube samples gave very similar spectral features (Figure 2S and Figure 4S in the Supporting Information). Therefore we suggest that high-speed centrifugation is necessary when using the r-SWNT samples.

Solutions for Hydrogen Peroxide-Related Experiments. A series of such buffered solutions of pH 6.0 were prepared with H_2O_2 concentrations ranging from 0 to 200 ppm. The H_2O_2 in a H_2O_2-reacted SDS−SWNT sample in buffered solution (about 0.3 mL) was dialytically removed by putting the sample in a dialysis membrane tube (6000−8000 MWCO, Spectrum Lab. Products, Inc.). The tube was then placed in a 500 mL beaker containing 300 mL of the buffer solution. The solution was stirred constantly during the dialysis process. In the first 2 h, the buffer solution was replaced with fresh buffer solution hourly. Under different dialysis times, the HiPco nanotube solution sample was taken out from the dialysis tube for optical absorption measurements and then placed back in the dialysis tube for further dialysis. Reversibility experiments with pH tuning were performed using 0.1 M NaOH and 0.1 M HCl solutions for pH titrations. The spectra were measured 15 min after the pH was adjusted. Control experiments were carried out with a mild oxidant, iodine, to elucidate SWNT interaction mechanisms with H_2O_2. Two additional SDS-encased HiPco nanotube solutions were prepared for this purpose. One contained 30 ppm I_2 and the other contained 45 ppm I_3^- (1.2×10^{-4} M) and 3000 ppm I^- ions (2.4×10^{-2} M). For reproducibility, all experiments were conducted at least twice.

The reactivity of HiPco nanotube suspensions encased by other surfactants including sodium dodecylbenzenesulfonate (SDBS) (1 wt %), cetyltrimethylammonium bromide (CTAB) (1 wt %), Triton X-100 (0.5 wt %), and sodium cholate (0.1 M) was also examined with hydrogen peroxide. We found that SWNTs encased with SDBS, CTAB, and Triton X-100 were insensitive to H_2O_2 under the same conditions used in this work. In cholate-dispersed HiPco nanotube suspensions, after addition of H_2O_2, white precipitate was observed, presumably due to the formation of an insoluble complex of cholate with H_2O_2. In addition, water-soluble HiPco and Tube@Rice nanotubes prepared by an acid oxidation method[9] became insensitive to H_2O_2. However, we observed that HiPco nanotubes encased in single-stranded DNA[15] and double-stranded DNA[17] had a similar optical response to H_2O_2 as that of the SDS-encased HiPco nanotubes shown in this work.

Optical and pH Measurements. The time-dependent optical absorption of the solutions was measured in 1 mm quartz cells using a Perkin-Elmer Lambda 19 UV−vis−NIR spectrometer.[40] SDS solutions in water or in pH 6.0 buffers without HiPco nanotubes were used as a reference for absorption background subtraction. MicroRaman measurements were conducted on the samples using a Renishaw microRaman 1000 spectrometer with 514 nm laser excitation from an Ar^+ laser and a 785 nm diode laser excitation source.[41] The spectra were calibrated with Si standards. The pH of the HiPco nanotube solutions was measured using an Orion model 420 pH meter with a Thermo Electron Orion micro pH glass electrode. No adsorption of SDS-encased SWNTs on the electrode was observed when rinsing it immediately after each pH measurement. The possible interference of SWNTs on pH measurements was also examined by comparing the pHs between a nanotube suspension in 1 wt % SDS solution and its filtrate after filtration. The pH is consistent within ±0.1, indicating minor SWNT interference on pH measurements in our conditions. All optical and pH measurements were conducted at room temperature.

Results and Discussion

Figure 1a shows a typical set of time-dependent absorption spectra of SDS-encased HiPco SWNTs in a pH 6.0 buffer after addition of 30 ppm H_2O_2. To correct the dilution effect on the spectral intensity caused by addition of H_2O_2, all spectra in this report are normalized to the S_{22} band at 659 nm, selected because it is insensitive to H_2O_2 or pH changes. The first and second interband transitions of semiconducting SWNTs (S_{11} and S_{22}) occur from 830 to 1360 nm and 600 to 830 nm, respectively.[10−18] The peak intensity at wavelengths <700 nm and between 930 and 1040 nm is insensitive to hydrogen peroxide. However, the spectral intensity decreases slightly with time between 700 and 930 nm and dramatically from 1040 to

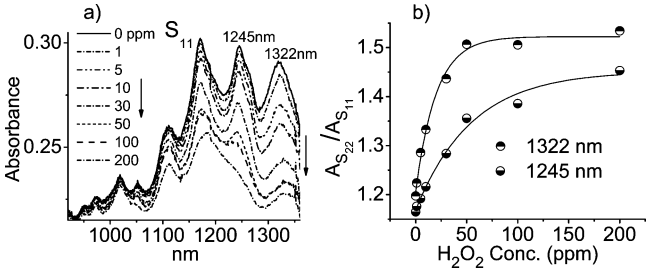

Figure 2. (a) Absorption spectra of SDS-encased HiPco SWNTs in pH 6.0 buffer solutions with changing H_2O_2 concentration. (b) The ratio As_{22}/As_{11} of the absorbance of the S_{11} (1245 and 1322 nm) and S_{22} (659 nm) bands of the SDS-encased SWNT samples changes as a function of H_2O_2 concentration.

1360 nm. Here we concentrate on the two most sensitive S_{11} bands with longer wavelengths, 1245 and 1322 nm, which correspond to larger diameter nanotubes.[42] The band at 1245 nm could be assigned to (10, 5) nanotubes with a diameter of 1.05 nm, which may overlap with corresponding bands from (9, 5), (10, 3), and (8, 7) nanotubes. The band at 1322 nm may come from (9, 7) nanotubes with a 1.1 nm diameter, which may overlap with bands from (12, 4) and (13, 2) nanotubes.[12,42] The intensity of the two S_{11} bands decays exponentially with the reaction time (only the 1322 nm band shown in Figure 1b). As shown in Figure 1b, the ratio As_{11} (1322 nm)/As_{22} (659 nm) decreases with time at different pHs. The observed spectral changes suggest strong electron withdrawal from the nanotube valence band by H_2O_2. At higher pH, the magnitude of the changes is smaller, suggesting the pH effects on the reactivity which will be further discussed later in the text.

The H_2O_2 concentration dependence was measured to determine the sensitivity. Figure 2a shows the absorption spectra of SDS-encased HiPco SWNTs in pH 6.0 buffer solutions with 0−200 ppm H_2O_2. The spectra were taken 1 h after mixing, and the spectral intensities were normalized to the intensity of the S_{22} band at 659 nm, which is insensitive to H_2O_2. The S_{11} band intensity decreases with increased H_2O_2 concentration. Figure 2b shows the H_2O_2 concentration-dependent absorbance of the S_{11} bands of 1245 and 1322 nm, plotted as the ratio of As_{22}/As_{11}. The ratio of both bands grows exponentially with H_2O_2 concentration. The ratio for the 1322 nm band intensity changes rapidly below 50 ppm but more slowly above 50 ppm, while the ratio for the 1245 nm band steadily grows until 200 ppm. The detection limit was 0.4 ppm (11 μM) for the 1322 nm band and 1 ppm (29 μM) for the 1245 nm band, respectively, based on a signal-to-noise ratio of 3. The sensitivity may be improved by optimizing the experimental conditions, which will be a subject for further investigation.

The recovery of spectral features was examined when the enzyme catalyst catalase was used to decompose the H_2O_2 into H_2O and O_2. SDS can denature enzymes such as catalase under certain conditions, but under other conditions it can even enhance the catalase activity.[43] In this case, the H_2O_2-suppressed optical absorption bands recovered upon catalase addition (Figure 3). The increase in spectral intensity under these conditions suggests that catalase decomposes the H_2O_2 in the SDS solution. Our preliminary test indicates that HiPco nanotubes can be solubilized in aqueous enzyme solutions with the assistance of mild sonication. Some proteins can be immobilized on SWNTs,[19,44,45] so catalase may coat the nanotubes by replacing SDS molecules whereupon it decomposes the H_2O_2.

The reversibility of the reaction of SDS-encased HiPco nanotubes with H_2O_2 was further demonstrated when the suppressed SWNT spectral features were fully regenerated by

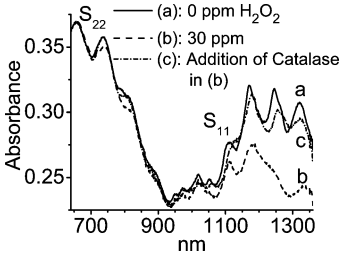

Figure 3. Recoverable optical absorption of an H_2O_2-interacted SDS−HiPco SWNT solution in pH 6.0 buffer after decomposing the H_2O_2 into H_2O and O_2 with catalase (140 units/mL).

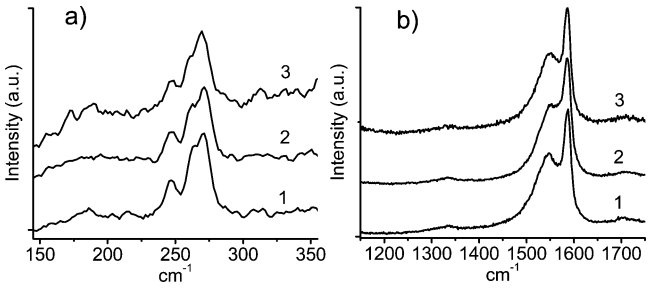

Figure 4. Raman spectra (excitation wavelength 514 nm) of an SDS−SWNT solution sample: (1) before addition of H_2O_2, (2) after addition of 50 ppm H_2O_2, and (3) after dialytically removing H_2O_2. The spectra were normalized using the main tangential mode at 1588 cm^{-1} and plotted on the same scale in each figure but shifted with equal division for clarity.

dialytically removing the H_2O_2 (Figure 5S in the Supporting Information). This demonstrates a very important advantage that SWNTs have for sensing applications; namely, they can be restored to their original condition.

Raman spectroscopy provides information on many aspects of a SWNT sample, including size distribution, disorder from defects or functionalization, and general electronic behaviors, so microRaman spectroscopy was used to analyze the H_2O_2-reacted samples with excitation sources of 514 and 785 nm. The 514 nm laser resonates predominantly with the electronic absorption bands of metallic nanotubes, while 785 nm resonates with the S_{22} bands of semiconducting nanotubes.[10,16,18] The Raman spectra from 514 nm laser excitation of a 50 ppm H_2O_2-reacted HiPco sample and one after dialytic removal of the H_2O_2 are largely the same as the spectrum before H_2O_2 addition. These features include the radial breathing mode (RBM) at about 150−300 cm^{-1} (Figure 4a), the tangential modes at 1500−1600 cm^{-1}, and the disorder (D) mode at 1330 cm^{-1} (Figure 4b).[41] The lack of change in the D mode upon H_2O_2 addition and after its removal indicates that the reaction with the H_2O_2 induces few defects in the metallic nanotubes. The Raman spectra of the same samples under 785 nm excitation in Figure 5b are complicated by S_{11} band gap fluorescence. The D mode at ~1300 cm^{-1} is partly obscured by fluorescence, which increases the background. However, the RBM modes are less affected by the fluorescence background as shown in Figure 5a. The peak intensity between 200 and 250 cm^{-1} decreases with addition of H_2O_2 and recovers after its removal. The peak intensity at 270 cm^{-1} belonging to (10, 2) nanotubes increases slightly with addition of H_2O_2, suggesting that either H_2O_2 induces spectral changes in the absorption bands of (10, 2) nanotubes that resonate with 785 nm or H_2O_2 causes additional bundle formation which enhances the (10, 2) nanotube Raman band.[16] The suppression and restoration are further confirmed from the Raman intensity ratio of the strongest peak at 237 cm^{-1} of (12, 1) nanotubes with the peak at 270 cm^{-1} of (10, 2) nanotubes. It changes from 3.85 before addition of H_2O_2 to 1.90

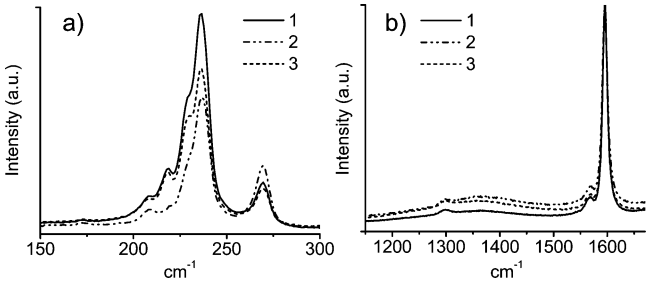

Figure 5. Raman spectra (excitation wavelength 785 nm) of the same SDS−SWNT solution sample in Figure 5: (1) before addition of H_2O_2, (2) after addition of 50 ppm H_2O_2, and (3) after dialytically removing H_2O_2. The spectra were normalized using the main tangential mode at 1588 cm^{-1}.

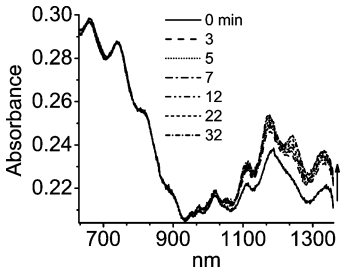

Figure 6. Absorption spectra of an SDS-encased HiPco SWNT solution containing 100 ppm H_2O_2 change as a function of time after adjusting the pH from 6 to 7.

after addition of H_2O_2, and returns to 3.25 after removal of the H_2O_2. The Raman results with 785 nm excitation are consistent with the absorption intensity changes around 785 nm in Figure 5S in the Supporting Information and further suggest the recoverability of the H_2O_2-reacted SDS−HiPco samples.

A recent paper suggests that oxygen forms covalent endoperoxides with SWNTs.[13] Protonation changes the endoperoxide into a hydroperoxide carbocation, which suppresses some SWNT spectral features. The absorption intensity recovers when the covalently bound oxygen is removed by increasing the pH.[13] In our work, H_2O_2 may follow a similar reaction mechanism by forming charge-transfer complexes with SDS-encased HiPco nanotubes and thus causing the observed spectral changes by altering the SWNT charge density.[13,14,16] H_2O_2 decreases the charge density on the SWNTs and so weakens the S_{11} bands.[9,13,14,16] More study of the detailed interaction mechanisms is required.

There are at least four possible factors behind the H_2O_2-induced spectral changes: (1) the high reduction potential of H_2O_2;[46] (2) the reaction of H_2O_2 with SDS;[47] (3) electrostatic interactions between negatively charged SDS micelles and HO_2^- at high pH;[48] and (4) hindrance of the polar H_2O_2 molecule's approach to SDS micelle-encased nanotubes. Electron withdrawal from SWNTs by H_2O_2 is related to its high reduction potential (standard reduction potential $E_0 = 1.763$ V).[46] It is intuitive that since pH changes the potential of H_2O_2, pH might be used to control electron withdrawal from SWNTs and hence their optical properties. The Nernst equation shows that the reduction potential (E) of H_2O_2 is 1.33 V at pH 6.0 and a concentration of 100 ppm (3.0×10^{-3} M). When the pH is increased to 10.0, E only drops to 1.09 V, which is still high enough to induce charge transfer from the nanotubes to the peroxide molecule and suppress spectral features as it does at pH 6.0. However, an increase in the solution pH actually restores the suppressed spectral features, as shown in Figures 6 and 7. As shown in Figure 6, the recovery of the suppressed spectral features of a 100 ppm H_2O_2-reacted SDS−HiPco nanotube

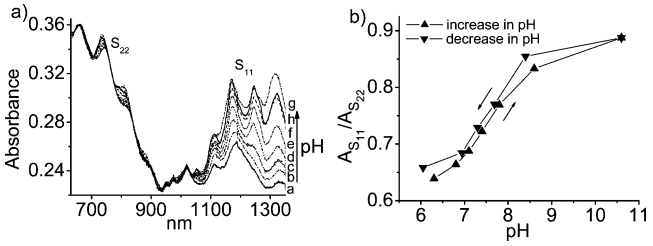

Figure 7. (a) Absorption spectra of an SDS-encased HiPco SWNT solution containing 100 ppm H_2O_2 at various pHs: (a) 6.3, (b) 6.8, (c) 7.1, (d) 7.4, (e) 7.8, (f) 8.6, (g) 10.6. The (h) curve (black solid line) is for the solution before H_2O_2 addition. (b) The ratio As_{11}/As_{22} of the absorbances of the S_{11} (1322 nm) and the S_{22} (659 nm) peaks of the same H_2O_2-containing sample responds reversibly to the pH changes.

sample is also time-dependent after the pH is adjusted to 7.0 from 6.0. The recovery process goes faster at higher pH. Figure 7a shows absorption spectra taken 15 min after the pH is adjusted for a 100 ppm H_2O_2-reacted SDS−HiPco nanotube sample at different pH values. The recovery of the spectral intensity is more complete with high pH. The result is in agreement with the observation in Figure 1b where the spectral intensity decrease is less at higher pH. In addition, the suppression and restoration is reversible with changing pH (Figure 7b). Three suppression and restoration cycles were performed with pH titrations, and the reversibility was always observed. Such reversibility undercuts the concern that H_2O_2 decomposes at high pHs under our conditions. These results suggest that the high reduction potential of H_2O_2 may not be the only factor involved in causing the observed spectral changes. The other factors listed above may also contribute.

A mild oxidant, iodine, with a relatively low standard reduction potential of 0.620 V in the aqueous I_2 form and 0.536 V in the I_3^- form[46] was used to test whether the high reduction potential of H_2O_2 dominated the spectral changes. Iodine is nonpolar, so it is expected that it would more easily approach the SDS-encased nanotubes than H_2O_2. Two aqueous iodine solutions were reacted with SDS−HiPco solutions: a 30 ppm aqueous iodine I_2 solution without I^- ions and a 45 ppm redox buffer solution containing both I_3^- (1.2×10^{-4} M) and I^- (2.4×10^{-2} M) ions. The iodine concentration is calculated as it is presented in the HiPco solutions. The reduction potential of the redox buffer solution containing I_3^- is calculated as 0.56 V, or about half of the H_2O_2 reduction potentials indicated above. Addition of the iodine in both the I_2 and I_3^- forms into the SDS−HiPco solutions at pH 6.0 similarly suppressed the nanotube spectral features within 10 min. Both I_2 and I_3^- produced similar spectral changes. Figure 7S in the Supporting Information shows the spectral changes induced in an SDS−HiPco solution by 30 ppm I_2. In contrast to H_2O_2, iodine also suppressed the spectral features between 930 and 1040 nm which are insensitive to H_2O_2. The suppressed features were restored by increasing the pH to 10.6, and were suppressed again as the pH was lowered to 6.0, just as occurred with H_2O_2 in Figure 7.[49]

The iodine results suggest that a high reduction potential is not the only factor causing the SWNT spectral changes. For example, they could also result when H_2O_2 reacts with SDS.[47] If SDS does compete with nanotubes to react with H_2O_2, then addition of more SDS into an H_2O_2-reacted SDS−HiPco sample may cause SWNT spectral changes, e.g., restoration of the S_{11} band intensity. However, as shown in Figure 6S in the Supporting Information, 10 times dilution with additional SDS solution in a H_2O_2-reacted SDS−HiPco sample does not change the S_{11} band intensity except for dilution. In addition, the iodine

results suggest that the H_2O_2−SDS reaction is also unlikely because iodine induces similar SWNT spectral changes even though it does not react with SDS under current conditions. It is therefore likely that both H_2O_2 and iodine form charge-transfer complexes with the nanotubes.[12,14] Iodine's nonpolarity may permit it to approach SDS-encased nanotubes more readily than H_2O_2 and thus accelerate the spectral changes. If, as recently suggested,[50] SDS adsorbs randomly on nanotube sidewalls, the H_2O_2 molecules can reach the nanotube surfaces by diffusion through the micelles, where they cause relatively slow spectral changes by charge transfer.

Recovery of the SWNT spectral features with increased pH may also reflect SDS deprotonation in more basic solutions, which changes the charge density on the SDS-encased nanotubes by refilling the valence band[7−9,13,14,16,51] and strengthens the optical transitions. In addition, at higher pH, the H_2O_2 converts to negatively charged HO_2^-, which is repelled from negatively charged SDS micelles.[48] The repulsion of the hydrogen peroxide restores the nanotubes and their spectral features to their original state. Furthermore, the interaction of SWNTs with O_2 dissolved in the solutions is also pH-dependent.[11,13,14,16] These pH-related effects may work simultaneously to restore or even strengthen the suppressed spectral intensity (Figure 7a).[39] Further experiments are underway to address the mechanisms so as to optimize the SWNT optical properties for applications.

In addition, there are increasing research activities about the toxicity of nanotubes. Our current study may provide some insights into possible contamination of nanotubes used for the research because the results shown in this work resemble those of nanotube suspensions prepared under strong sonication.[39] The byproducts of sonication may include oxidative nitric and nitrous acids and hydrogen peroxide which may form charge-transfer complexes with SWNTs and suppress the SWNT spectral intensity.[39] When a suspension prepared with sonication is used in the toxicity research, caution has to be taken to ensure that the byproducts of sonication are removed so that the nature of pristine SWNTs can be evaluated. The removal of the byproducts can be done by using dialysis as demonstrated in this work. Otherwise, the conclusions regarding nanotube toxicity might be complicated by the presence of sonication-generated oxidative byproducts.

Conclusions

The unique SWNT optical sensitivity to H_2O_2 may lead to new nanotubes-based optical tools for study of the physiological and pathological roles of H_2O_2 in living organisms. Enzyme-immobilized SWNTs are potential sensors to detect biologically important target analytes by molecular recognition if the enzymatic products include hydrogen peroxide. As a demonstrating example among numerous potential applications based on the H_2O_2 findings, water-soluble SDS-encased SWNTs immobilized with glucose oxidase can be used to optically detect glucose at a detection limit of 0.02 mM.[52] The optical properties of nanotubes thus hold out great promise for applications.

Acknowledgment. We thank Virang Patel for his assistance.This work was supported by ARO under Award No. DAAD 190210140, ONR, and DTRA.

Supporting Information Available: Figure 1S, a TEM image of the raw HiPco nanotube sample; Figure 2S, time-dependent absorption spectra of 10 ppm H_2O_2-reacting SDS−SWNTs prepared by a high-speed centrifuge in a pH 6.0 buffer solution; Figure 3S, absorption spectra showing SWNT suspension stability; Figure 4S, centrifuge speed-dependent absorption spectra of suspensions of a new raw HiPco nanotube sample; Figure 5S, dialytic removal of H_2O_2 and spectral recovery of a H_2O_2-reacted SWNT sample; Figure 6S, dilution effect on a H_2O_2-reacted SDS−SWNT sample; Figure 7S, spectral changes of an iodine-reacting SWNT suspension. This material is available free of charge via the Internet at http://pubs.acs.org.

References and Notes

(1) Chen, R. J.; Bangsaruntip, S.; Drouvalakis, K. A.; Kam, N. W. S.; Shim, M.; Li, Y.; Kim, W.; Utz, P. J.; Dai, H. *Proc. Natl. Acad. Sci. U.S.A.* **2003**, *100*, 4984−4989.

(2) An, L.; Fu, Q.; Lu, C.; Liu, J. *J. Am. Chem. Soc.* **2004**, *126*, 10520−10521.

(3) Besteman, K.; Lee, J.-O.; Wiertz, F. G. M.; Heering, H. A.; Dekker, C. *Nano Lett.* **2003**, *3*, 727−730.

(4) Star, A.; Lu, Y.; Bradley, K.; Gruner, G. *Nano Lett.* **2004**, *4*, 1587−1591.

(5) Lin, Y.; Lu, F.; Tu, Y.; Ren, Z. *Nano Lett.* **2004**, *4*, 191−195.

(6) Wang, J.; Deo, R. P.; Poulin, P.; Mangey, M. *J. Am. Chem. Soc.* **2003**, *125*, 14706−14707.

(7) Itkis, M. E.; Niyogi, S.; Meng, M. E.; Hamon, M. A.; Hu, H.; Haddon, R. C. *Nano Lett.* **2002**, *2*, 155−159.

(8) Chen, J.; Hamon, M. A.; Hu, H.; Chen, Y.; Rao, A. M.; Eklund, P. C.; Haddon, R. C. *Science* **1998**, *282*, 95−98.

(9) Zhao, W.; Song, C.; Pehrsson, P. E. *J. Am. Chem. Soc.* **2002**, *124*, 12418−12419.

(10) O'Connell, M. J.; Bachilo, S. M.; Huffman, C. B.; Moore, V. C.; Strano, M. S.; Haroz, E. H.; Rialon, K. L.; Boul, P. J.; Noon, W. H.; Kittrell, C.; Ma, J.; Hauge, R. H.; Weisman, R. B.; Smalley, R. E. *Science* **2002**, *297*, 593−596.

(11) Strano, M. S.; Huffman, C. B.; Moore, V. C.; O'Connell, M. J.; Haroz, E. H.; Hubbard, J.; Miller, M.; Rialon, K.; Kittrell, C.; Ramesh, S.; Hauge, R. H.; Smalley, R. E. *J. Phys. Chem. B* **2003**, *107*, 6979−6985.

(12) Ostojic, G. N.; Zaric, S.; Kono, J.; Strano, M. S.; Moore, V. C.; Hauge, R. H.; Smalley, R. E. *Phys. Rev. Lett.* **2004**, *92*, 117402.

(13) Dukovic, G.; White, B. E.; Zhou, Z.; Wang, F.; Jockusch, S.; Steigerwald, M. L.; Heinz, T. F.; Friesner, R. A.; Turro, N. J.; Brus, L. E. *J. Am. Chem. Soc.* **2004**, *126*, 15269−15276.

(14) Zheng, M.; Diner, B. A. *J. Am. Chem. Soc.* **2004**, *126*, 15490−15494.

(15) Zheng, M.; Jagota, A.; Semke, E. D.; Diner, B. A.; Mclean, R. S.; Lustig, S. R.; Richardson, R. E.; Tassi, N. G. *Nat. Mater.* **2003**, *2*, 338−342.

(16) O'Connell, M. J.; Eibergen, E. E.; Doorn, S. K. *Nat. Mater.* **2005**, *4*, 412−418.

(17) Kelley, K.; Pehrsson, P. E.; Ericson, L. M.; Zhao, W. *J. Nanosci. Nanotechnol.* **2005**, *5*, 1029−1032.

(18) Strano, M. S.; Dyke, C. A.; Usrey, M. L.; Barone, P. W.; Allen, M. J.; Shan, H.; Kittrell, C.; Hauge, R. H.; Tour, J. M.; Smalley, R. E. *Science* **2003**, *301*, 1519−1522.

(19) Barone, P. W.; Baik, S.; Heller, D. A.; Strano, M. S. *Nat. Mater.* **2005**, *4*, 86−92.

(20) Cherukuri, P.; Bachilo, S. M.; Litovsky, S. H.; Weisman, R. B. *J. Am. Chem. Soc.* **2004**, *126*, 15638−15639.

(21) O'Connell, M. J.; Boul, P.; Ericson, L. M.; Huffman, C.; Wang, Y.; Haroz, E.; Kuper, C.; Tour, J.; Ausman, K. D.; Smalley, R. E. *Chem. Phys. Lett.* **2001**, *342*, 265−271.

(22) Steuerman, D. W.; Star, A.; Narizzano, R.; Choi, H.; Ries, R. S.; Nicolini, C.; Stoddart, J. F.; Heath, J. R. *J. Phys. Chem. B* **2002**, *106*, 3124−3130.

(23) Star, A.; Steuerman, D. W.; Heath, J. R.; Stoddart, J. F. *Angew. Chem., Int. Ed.* **2002**, *41*, 2508−2512.

(24) Bandyopadhyaya, R.; Nativ-Roth, E.; Regev, O.; Yerushalmi-Rozen, R. *Nano Lett.* **2002**, *2*, 25−28.

(25) Pompeo, F.; Resasco, D. E. *Nano Lett.* **2002**, *2*, 369−373.

(26) Turner, A. P. F., Karube, I., Wilson, G. S., Eds. *Biosensors: Fundamentals and Applications*; Oxford University Press: New York, 1987.

(27) Henry, C. M. *Anal. Chem.* **1998**, *70*, 594A−598A.

(28) Rhodes, R. K.; Shults, M. C.; Updike, S. J. *Anal. Chem.* **1994**, *66*, 1520−29.

(29) Wang, J.; Zhang, X. *Anal. Chem.* **2001**, *73*, 844−847.

(30) Bindra, D. S.; Zhang, Y.; Wilson, G. S.; Sternberg, R.; Thevenot, D. R.; Moatti, D.; Reach, G. *Anal. Chem.* **1991**, *63*, 1692−96.

(31) Gough, D. A.; Lucisano, J. Y.; Tse, P. H. S. *Anal. Chem.* **1985**, *57*, 2351−57.

(32) Csoregi, E.; Schmidtke, D. W.; Heller, A. *Anal. Chem.* **1995**, *67*, 1240−44.

(33) Liu, J.; Rinzler, A. G.; Dai, H.; Hafner, J. H.; Bradley, R. K.; Boul, P. J.; Lu, A.; Iverson, T.; Shelimov, K.; Huffman, C. B.; Rodriguez-Macias, F.; Shon, Y.; Lee, T. R.; Colbert, D. T.; Smalley, R. E. *Science* **1998**, *280*, 1253−1256.

(34) Chang, M. C. Y.; Pralle, A.; Isacoff, E. Y.; Chang, C. J. *J. Am. Chem. Soc.* **2004**, *126*, 15392−15393.

(35) Huang, M. H.; Mao, S.; Feick, H.; Yan, H.; Wu, Y.; Kind, H.; Weber, E.; Russo, R.; Yang, P. *Science* **2001**, *292*, 1897−1899.

(36) Law, M.; Sirbuly, D. J.; Johnson, J. C.; Goldberger, J.; Saykally, R. J.; Yang, P. *Science* **2004**, *305*, 1269−1273.

(37) Tong, L.; Gattass, R. R.; Ashcom, J. B.; He, S.; Lou, J.; Shen, M.; Maxwell, I.; Mazur, E. *Nature* **2003**, *426*, 816−819.

(38) Kasili, P. M.; Song, J. M.; Vo-Dinh, T. *J. Am. Chem. Soc.* **2004**, *126*, 2799−2806.

(39) Benedict, B.; Pehrsson, P. E.; Zhao, W. *J. Phys. Chem. B*, **2005**, *109*, 7778−7780.

(40) Zhao, W.; Song, C.; Zheng, B.; Liu, J.; Viswanathan, T. *J. Phys. Chem. B* **2002**, *106*, 293−296.

(41) Pehrsson, P. E.; Zhao, W.; Baldwin, J. W.; Song, C.; Liu, J.; Kooi, S.; Zheng, B. *J. Phys. Chem. B* **2003**, *107*, 5690−5695.

(42) Weisman, R. B.; Bachilo, S. M. *Nano Lett.* **2003**, *3*, 1235−1238.

(43) Mosavi-Movahedi, A. A.; Jones, M. N.; Pilcher, G. *Int. J. Biol. Macromol*. **1988**, *10*, 75−78.

(44) Azamian, B. R.; Davis, J. J.; Coleman, K. S.; Bagshaw, C. B.; Green, M. L. H. *J. Am. Chem. Soc.* **2002**, *124*, 12664−12665.

(45) Karajanagi, S. S.; Vertegel, A. A.; Kane, R. S.; Dordick, J. S. *Langmuir* **2004**, *20*, 11594−11599.

(46) Harris, D. C. *Exploring Chemical Analysis*, 3rd ed.; W. H. Freeman and Company: New York, 2004.

(47) Ponganis, K. V.; De Araujo, M. A.; Hodges, H. L. *Inorg. Chem.* **1980**, *19*, 2704−2709.

(48) Jankovic, I. A.; Cakar, M. M.; Nedeljkovic, J. M. *J. Serb. Chem. Soc.* **1999**, *64*, 359−364.

(49) The pH-induced spectral restoration with the iodine−SDS−nanotube system may originate from the same causes as it does in the H_2O_2−SDS−nanotube system, but with additional complications due to the possible iodine disproportion to hypoiodous acid (HOI), iodate (IO_3^-), and iodide at high pH.[46] Details of the iodine-related results are to be reported elsewhere.

(50) Yurekli, K.; Mitchell, C. A.; Krishnamoorti, R. *J. Am. Chem. Soc.* **2004**, *126*, 9902−9903.

(51) Cui, Y.; Wei, Q.; Park, H.; Lieber, C. M. *Science* **2001**, *293*, 1289−1292.

(52) Song, C.; Pehrsson, P. E.; Zhao. W. Unpublished work, 2004.